On the Non-Intrusive Extraction of Residents' Privacy and Security Sensitive Information from Energy Smart Meters

Pascal Schirmer and Iosif Mporas
Communications and Intelligent Systems Group
School of Engineering and Computer Science, University of Hertfordshire
Hatfield AL10 9AB, UK
{p.schirmer, i.mporas}@herts.ac.uk

Abstract:

Energy smart meters have become very popular in monitoring and smart energy management applications. However, the acquired measurements except the energy consumption information may also carry information about the residents' daily routine, preferences and profile. In this article we investigate the potential of extracting information from smart meters related to residents' security and privacy sensitive information. Specifically, using methodologies for load demand prediction, non-intrusive load monitoring and elastic matching, evaluation of extraction of information related to house occupancy, multimedia watching detection, socioeconomic and health profiling of residents was performed. The evaluation results showed that the aggregated energy consumption signals contain information related to residents' privacy and security, which can be extracted from the smart meter measurements.

Keywords: consumer privacy, home security, smart meters, non-intrusive load monitoring.

1. Introduction

In the last decade smart meters have been extensively employed in consumer households, with 60% of the houses in the United States [1] and 50% of the houses in Europe [2] having smart meters installed. Based on the additional information, in the form of the aggregated energy consumption as measured by the smart meter, several techniques within the area of Information and Communication Technology (ICT) have been proposed. For example, smart meter data have been used for load scheduling, managing or rescheduling the usage of devices in order to reduce electricity bills [3], e.g. by using some appliances like washing machines at night time during which electricity costs are usually lower [4]. Conversely, smart meter data are also utilized by energy companies in order to estimate grid load and to build accurate models for long-term and short-term load forecasting [5, 6].

In detail, smart meters, also referred to as smart plugs, are devices used to measure electrical power/energy consumption with resolution in the order of seconds to minutes. Smart meters measure the voltage-drop over the device/circuit and the current flowing through the device/circuit with an arbitrary sampling frequency f_s which usually varies from 1⁄60 Hz to 30 kHz [7]. Higher sampling frequencies are usually preferred, since they contain more detailed information about the energy consumption, however they increase linearly the amount of acquired data and exponentially the cost of hardware [8]. With the sampling rate in the order of seconds data handling for several months/years becomes feasible and hardware costs are relatively low. Specifically, two different smart metering configurations are possible to monitor the energy consumption of a household or building on device level. First, using only one smart meter to measure the aggregated energy consumption of a household and applying signal separation methods to determine the consumption per appliance, which is referred to as a Non-Intrusive Load Monitoring (NILM) [9]. Conversely, in Intrusive Load Monitoring (ILM) one smart meter per device is used, thus measuring the energy consumption directly and separately for each device. Compared to ILM, NILM has the advantage of requiring less hardware (ILM uses one smart meter per device which is impractical for most households) as well as meets consumers' acceptability with respect to privacy conserving [10, 11].

However, even when just measuring the aggregated signal, the ability to provide real-time information through smart-metering and determining detailed household energy consumption, rises consumers' privacy and security concerns and makes energy data protection prominent [12, 13]. To address these issues, energy monitoring must be carried out cost effectively and under the consideration of privacy and security concerns. Specifically, in [14] exploiting occupancy related information as well as location tracking within a household smart meters were identified as a sever information leak when using high-frequency smart metering. In order to increase the security of smart metering systems with respect to extraction of events and thus estimation of occupancy, location and activity in a household, several approaches have been proposed in literature. Specifically, detailed issues of smart metering within consumer homes and smart grid architectures have been presented in [15, 16]. Accordingly, software and hardware based solutions have been presented through protocols identifying trusted smart meters [12], smoothing patterns and minimization of mutual information based on local storages [17].

Extraction of residents' individual information from smart meters has been studied in the bibliography. For example in some approaches the smart meter data is utilized for occupancy estimation and accurate tracking of a person's location within their house, e.g. by detecting changes of lighting or other frequently used devices [14]. Furthermore, estimation of working routines and number of people living in a household has been evaluated [12, 14]. Additionally, smart meters have been used for identification of multi-media content and TV channel estimation, both from isolated device signals [18] and from the aggregated smart meter signal [19]. Moreover, concepts for e-health monitoring based on smart-meter data have been proposed recently [20].

With smart-meters being able to be utilized in extraction of residents' individual information, as described above, extraction of security relevant information has been studied as residents are concerned about the protection of their private information, i.e. occupancy or routines [21]. Specifically, in [22] a machine learning based solution utilizing Random Forests (RF) as classifier for occupancy detection is presented. Furthermore, the approaches in [23, 24] present advanced occupancy estimations for limited ground truth data [23] and under consideration of renewable energy generation within the same household [24]. Moreover, an extensive comparison of machine learning classifiers with optimal hyperparameters was presented in [25]. Additionally, a general review of information extraction from smart meters is given in [26], while extraction of employment status based on energy consumption was presented in [27]. In view of that , to prevent the extraction of information filtering approaches, mainly based on large energy storages, have been proposed. In specific, the approach presented in [28] proposes a thermal energy storage, while the work in [29] compares different chemical storages on their capability to filter the energy consumption signal.

In this article we investigate if and how accurately smart meters can be used to estimate information about household residents' profile and their daily indoors activities and habits as well as how much dangerous these extracted data are if they fall in the wrong hands in terms of invade of privacy and threaten of security. In detail, four different scenarios have been evaluated, namely occupancy estimation through either load forecasting or non-intrusive load monitoring, multimedia content identification and extraction of socio-economic and health-related information. The remainder of this paper is organized as follows. In Section 2 a high-level conceptual architecture for non-intrusive information extraction based on smart meters is described. In Section 3 evaluation of different types of extraction of residents' privacy and security sensitive information are presented. Finally, discussion and conclusion are provided in Section 4.

2. Non-Intrusive Home Information Extraction Architecture using Smart Meters

The extraction of information related to the privacy and the security of individuals, residents of a house, using a non-intrusive setup is discussed in this Section. The conceptual block diagram for extraction of information based on the aggregated energy consumption measurements of an NILM setup is illustrated in Fig. 1.

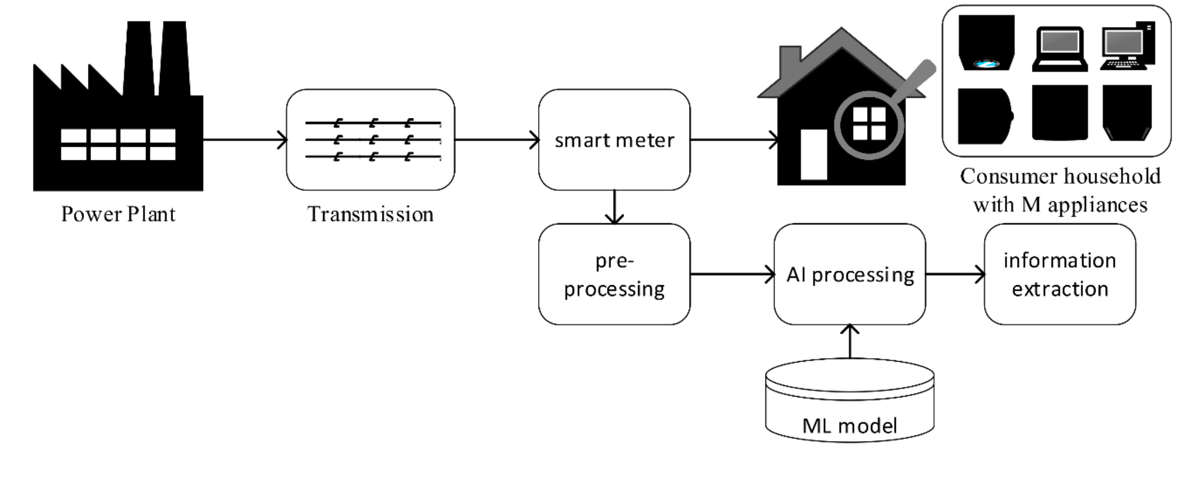

Fig. 1: Conceptual block diagram for extraction of information based on the aggregated energy consumption measurements, including a power plant, a transmission channel and a consumer household with M appliances. Additionally, the total power consumption of the household is measured by a single smart meter and processed by AI algorithms. Based on a set of machine learning models information extraction within the household is performed.

As shown in Fig. 1 the high-level grid architecture is transferring energy from a power plant to a consumer household consisting of a set of M appliances. In this architecture a single smart meter is used in order to measure the aggregated power consumption with sampling period in the order of 30 minutes up-to 1 second. Based on the aggregated measurements, several machine learning and Artificial Intelligence (AI) based algorithms have been proposed in literature in order to extract information or detect events and patterns "hidden" in the energy consumption signal of a household. Specifically, three popular methods to process the extracted information are load prediction [30], Non-Intrusive Load Monitoring [9] and elastic matching [31].

As regards load prediction, it is used for ahead prediction of energy values and thus was evaluated for a wide range of application including, grid stability [4], demand side management [32, 33] and optimal usage of local storages [34, 35]. In the NILM task the aim is to extract the power consumption per appliance based on the aggregated measurements [9], thus investigating the usage patterns and activity of certain devices within a household [36] in order to perform load management and demand shifting. However, as usage patterns are extracted NILM operation has raised privacy and security questions, thus an architecture trying to minimize mutual information was proposed in [35]. Regarding elastic matching algorithms, Dynamic Time Warping (DTW) [37] and Multi Variance Matching (MVM) [31] have been proposed in order to find similarities between the measured smart meter signal and a set of reference signals, thus also attempting to extract information. In addition, the extraction of appliance activations for the NILM case has been considered in [31] as well as the identification of different TV channels in [19].

Despite the above mentioned previous works, there is no smart meter based setup in the literature describing the capabilities of smart metering technology in extracting residents' individual privacy-sensitive and security-threating information, as for example the social class of residents and consequently their living conditions and habits, based on their aggregate energy consumption data. We deem the conceptual block diagram of Fig. 1 to serve as a testbed architecture for evaluating the privacy and security issues raised by the use of energy smart meters mainly in households as well as in other types of buildings.

3. Experimental Evaluation

The experimental evaluation to investigate if and how accurately smart meters can be used to estimate information about household residents' profile and their daily indoors activities and habits, according to the conceptual diagram presented in Section 2, is based on the block diagram shown in Fig. 2.

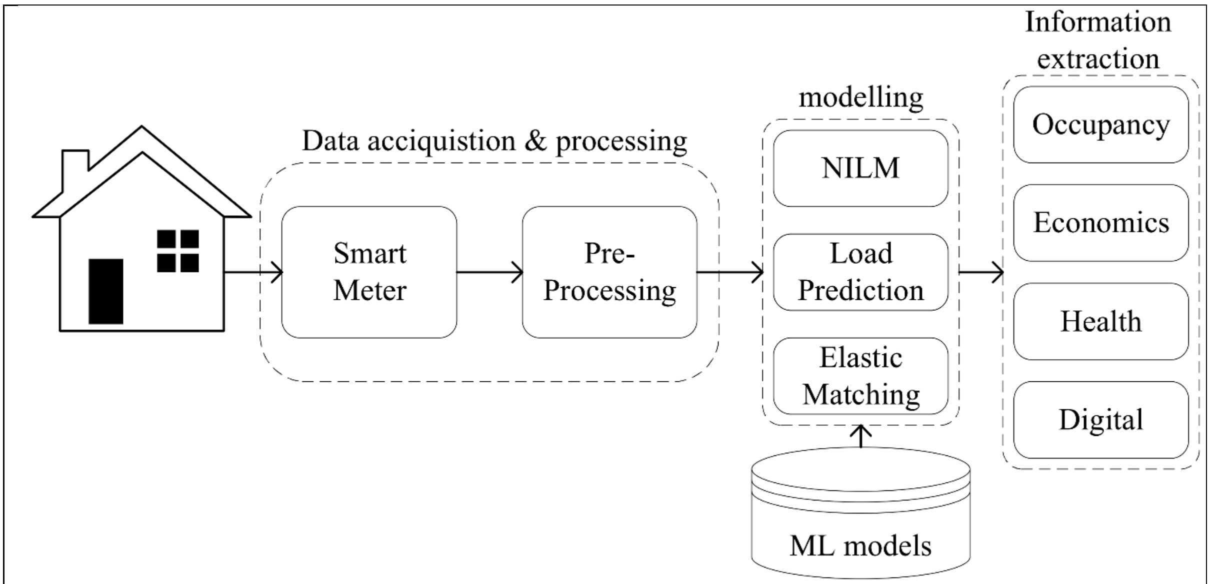

Fig. 2: Block diagram of the proposed experimental evaluation based on the aggregated power consumption of a household. Based on the three algorithms NILM, load prediction and elastic matching, information regarding occupancy, economic data, health data and digital information are extracted.

As illustrated in Fig. 2 the generalized architecture for extraction of residents' information consists of three main stages, namely data acquisition including relevant pre-processing, modelling and information extraction. In this work three AI based techniques, namely NILM, load prediction and elastic matching, are utilized in order to build models used for extraction of information. Specifically, information regarding four categories, namely occupancy, economics, health and digital based features is extracted.

In order to evaluate the performance of the different approaches, five different accuracy metrices are used. In detail, three metrices will be used in order to evaluate regression-based models, namely the Mean Absolute Error (MAE), the Root Mean Square Error (RMSE) and the Pearson correlation coefficient R, as defined in Eq. 1 to Eq. 3:

$$MAE = \frac{1}{T}\sum_{t=1}^{\mathrm{T}} |x_t - \hat{x}_t| \tag{1}$$

$$RMSE = \sqrt{\frac{\sum_{t=1}^{\mathrm{T}} (x_t - \hat{x}_t)^2}{T}} \tag{2}$$

$$R = \frac{\sum_{t=1}^{T} (x_t - \bar{x})(\hat{x}_t - \bar{\hat{x}})}{\sqrt{\sum_{t=1}^{T} (x_t - \bar{x})^2} \cdot \sqrt{\sum_{t=1}^{T} (\hat{x}_t - \bar{\hat{x}})^2}} \tag{3}$$

where x_t is the ground-truth value of an arbitrary variable at time step t, $\hat{x}_t$ is the model prediction and $\bar{x}$ and $\bar{\hat{x}}$ are the mean values of x and $\hat{x}$, respectively.

While for the case of classification-based approaches two different accuracy metrices are used, namely the classification Accuracy (ACC) and the F_1-score (F_1) respectively, as defined in Eq. 4 and Eq. 5:

$$ACC = \frac{TP + TN}{TP + TN + FP + FN} \tag{4}$$

$$F_1 = 2 \cdot \frac{TP}{2 \cdot TP + FN + FP} \tag{5}$$

where TP are the True Positives, TN are the True Negatives, FP are the False Positives and FN are the False Negatives respectively.

3.1. Occupancy Estimation through Load Forecasting

As discussed in Section 2 occupancy information for a household is a privacy and security sensitive information and we investigated if it can be extracted with sufficiently high accuracy from the aggregated signal of a household or building. The evaluated architecture for occupancy estimation based on load forecasting is illustrated in Fig. 3.

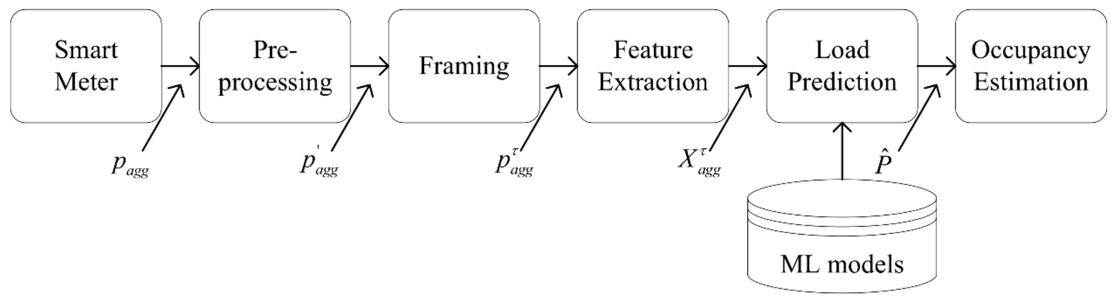

Fig. 3: Block diagram of the evaluated architecture for occupancy estimation based on load prediction.

As illustrated in Fig. 3 the architecture consists of a smart meter measuring the aggregated power consumption p_{agg}, pre-processing (e.g. down-sampling or filtering) transforming the aggregated signal to p'_{agg}, framing (p^{τ}_{agg}), feature extraction transforming the frame to a multi-dimensional feature vector X^{τ}_{agg}, load prediction giving an estimate for the power consumption $\hat{p}_{agg}$, and a rule based algorithm for the occupancy estimation. The ahead prediction of an energy consumption sample w of a target house m of the community can be defined as:

$$\hat{p}^{m}_{agg}(t+w) = r_{\theta}(p^{m}_{agg}(t_0{:}\, t)) \quad (6)$$

where $[t_0{:}\, t]$ is the previous time interval used to predict the w^{th} samples ahead $(t+w)$, $p^{\mathrm{m}}_{agg}(t_0{:}\, t) \in \mathbb{R}^{(t-t_0+1)}$ is the energy consumption of the previous time window, $\hat{p}^{m}_{agg}(t+w) \in \mathbb{R}^{1}$ its step-ahead prediction of the w^{th} sample and $r(\cdot)$ a regression model (e.g. Linear Regression (LR), Support Vector Regression (SVR), Long Short Term Memory (LSTM), etc.) with a set of free parameters θ.

We expect that across different households in the community there are common energy consumption trends and motifs as well as interdependencies due to potential socioeconomic similarities or in between them social relationships, which potentially have time lags between them or appear simultaneously [38]. This motivates us to use the energy consumption history of $M-1$ other households as an additional input of information to enhance the prediction of energy load demand of the target house, similarly to the architecture we proposed in [39]. In that case the formalization of the problem is expressed as:

$$\hat{p}_{agg}^{m}(t+w) = r_\theta(p_{agg}^{m}(t_0{:}\,t), p_{agg}^{m}(t_0{:}\,t)) \quad \text{with } 1 \leq m < (M-1) \tag{7}$$

with $p_{agg}^{\mathrm{m}}(t_0{:}\,t)$ being the energy consumption signal in the time window $[t_0{:}\,t]$ for the m^{th} neighboring household of the community. Given that prediction models are trained from several households' data, the use of socioeconomic information of the consumers of the target house would result in load demand forecasting models adapted to the characteristics of each socioeconomic group of consumers. Socioeconomic information enhanced models are expected to predict more precisely the energy consumption behaviour of a house [39, 40] and the prediction can be formalized as:

$$\hat{p}_{agg}^{m}(t+w) = r_\theta(p_{agg}^{m}(t_0{:}\,t), p_{agg}^{m}(t_0{:}\,t), s_m) \quad \text{with } 1 \leq m < (M-1) \tag{8}$$

where $s_m \in \mathbb{R}^K$ is the K-dimensional socioeconomic information of the target house.

To evaluate the presented architecture the publicly available dataset "Smart Meters in London" (SMinL) [41] was used, utilizing population, housing finance, transport and environment as socioeconomic features similarly as in [39]. Specifically, for our evaluation the year 2013 was used, since year 2012 has several gaps in the measurements, using 50 households per ACRON group, thus a total of 700 households. Furthermore we excluded ACRON-{B, K, M} as they have missing samples in the selected time interval. Especially, according to the setups described in Eq. 6-8 three different experimental protocols will be evaluated, referred to as Baseline (BL) as described in Eq. 6, Inter-Household (IH) as described in Eq. 7 and Socio-Economic (SO) as described in Eq. 8. The regression function $r_\theta(\cdot)$ will be modelled through an LSTM consisting of two layers with 16 nodes per layer and hyperbolic tangents (tanh) as activation functions. The free parameters were determined on a bootstrap training dataset utilizing grid search [39]. The results for the three different experimental protocols and up to W=48 samples (i.e. up to 1 day ahead) ahead prediction is evaluated in terms of MAE and are illustrated in Fig. 4.

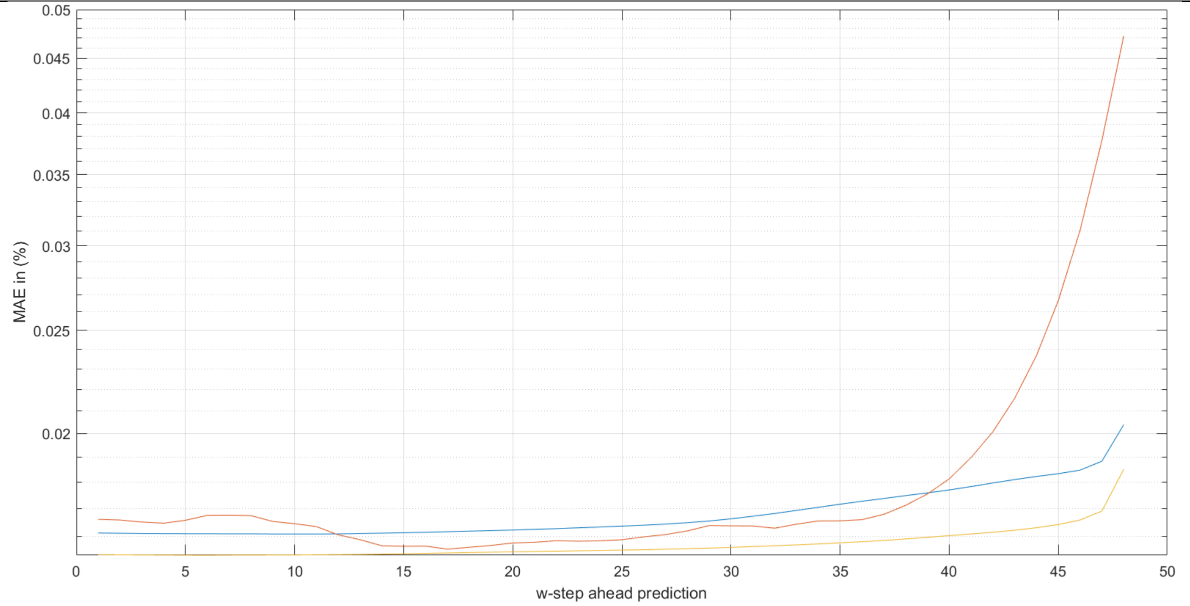

Fig. 4. Load predictions for different number of steps ahead predictions and different load prediction scenarios: baseline, inter household and socio-economic. Step ahead prediction is measured in samples per half hour.

As can be seen in Fig. 4 the IH and SO protocols significantly outperform the baseline system. In detail, for step ahead greater than 40 samples (i.e. 20 hours) the prediction error of the baseline system increases to 5%, while the IH and SO protocols retain the error below 2%.

Based on an accurate ahead prediction of energy consumption occupancy information extraction can be performed, especially two different approaches can be thought of. First, based on the ahead prediction patterns or time intervals can be found where consumption is low, thus a set of rule-based methods or thresholds can be applied in order to obtain occupancy information. Second, based on the changes in predicted energy consumption a second Machine Learning (ML) based predictor could be utilized in order to classify time frames of predicted energy consumption.

3.2. Occupancy Prediction through Device Operation Identification

Next to the possibility of extracting occupancy information based on ahead prediction of the aggregated load as discussed in Section 3.1, NILM can be utilized to perform occupancy identification based on device operation. In the NILM task the energy consumption measurements of one sensor are disaggregated on device level, within time windows (frames) [42]. Specifically, for a set of $M-1$ known devices each consuming power p_m with $1 \leq m \leq M$, the aggregated power p_{agg} measured by the sensor will be:

$p_{agg} = f(p_1, \ldots, p_{M-1}, g) = \sum_{m=1}^{M-1} p_m + g = \sum_{m=1}^{M} p_m$	(9)

where $g = p_M$ is a 'ghost' power consumption (noise) usually consumed by one or more unknown devices and $f(\cdot)$ is the aggregation function. In NILM the goal is to find estimations, $\hat{p}_m$ and $\hat{g} = \hat{p}_M$, of the power consumption of each device m using a disaggregation function $f^{-1}(\cdot)$ with minimal estimation error, i.e.

$\hat{P} = \{\hat{p}_1, \hat{p}_2, \ldots, \hat{p}_{M-1}, \hat{g}\} = f^{-1}(p_{agg})$	(10)
$\underset{f^{-1}}{\operatorname{argmin}}\{\left(p_{agg} - \sum_{1}^{M} \hat{p}_m\right)^2\}$	

In order to map the appliances estimates $\hat{P}$ to a set of binary appliance states $\hat{S} = \{\hat{s}_1, \hat{s}_2, \ldots, \hat{s}_{M-1}, \hat{s}_M\}$, thresholding is applied separately for each appliance estimate $\hat{p}_m$ as defined in Eq. 11.

$\hat{s}_m = \theta(\hat{p}_m) = \begin{cases} 1 & if\ \hat{p}_m \geq \theta \\ 0 & if\ \hat{p}_m < \theta \end{cases}$	(11)

The block diagram of the proposed NILM architecture for occupancy estimation is illustrated in Fig. 5.

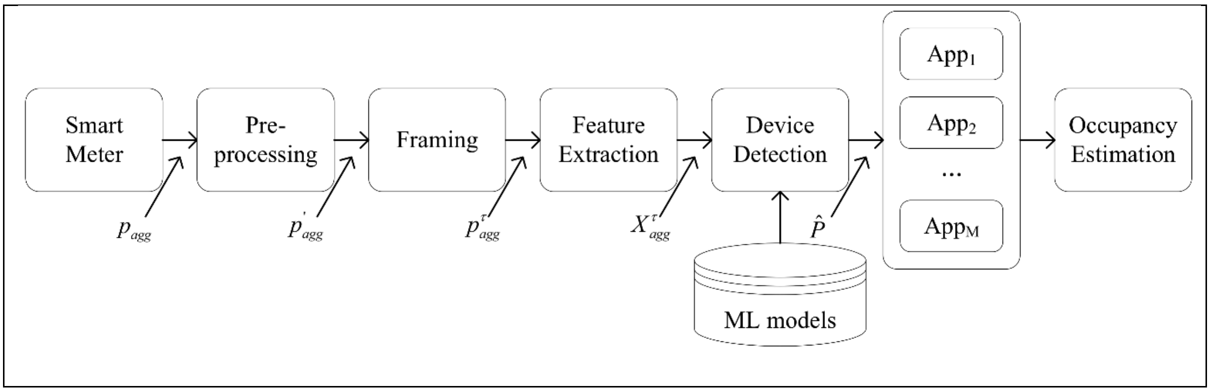

Fig. 5: Block diagram of the proposed architecture for occupancy estimation based on NILM. In detail the model consists of pre-processing, framing, feature extraction, load prediction and occupancy estimation.

In detail, the architecture illustrated in Fig. 5 consists of pre-processing, framing, feature extraction, device detection and occupancy estimation based on the device operation. In detail, for the device estimation stage two different ML models have been evaluated, namely a LSTM architecture and a CNN architecture [43]. The layer structure and the free parameters for both architectures can be found in Table I.

TABLE 1: LAYER STRUCTURE FOR NILM ARCHITECUTRE FOR LSTM AND CNN NETWORK STRUCTURES RESPECTIVELY. COVOLUTIONAL LAYERS ARE OF THE FORM CONV2D (#-FILTERS, KERNEL, PADDING, STRIDES, ACTIVATION)

Layer number	LSTM	CNN [43]
1	Input(64, 1, 1)	Input(64, 1, 1, 1)
2	LSTM(128, sequences=True)	Conv2d(30,10,'same',1, relu)
3	LSTM(256)	Conv2d(30,8,'same',1, relu)
4	Dense(128, activation='tanh')	Conv2d(40,6,'same',1, relu)
5	Dense(1, activation='linear')	Conv2d(50,5,'same',1, relu)
6	-	Conv2d(50,5,'same',1, relu)
7	-	Flatten
8	-	Dense(1024, activation='relu')
9	-	Dense(1, activation='linear')

As illustrated in Table 1 both the LSTM and the CNN structure take time frames of size 64 as input, while the core of the architectures consists of LSTM layers and CNN layers respectively. Additionally, each architecture has a dense layer at the end using a linear function as activation.

In order to evaluate the proposed architecture, house two of the publicly available Reference Energy Disaggregation Data (REDD) dataset was used for evaluation. In detail, the first half of the dataset was used for training and the second half for testing, while the threshold of an appliance activation was set to 50 W equally across all appliances. The results for both architecture as well as for ACC and F_1 score are tabulated in Table 2.

TABLE 2: NILM RESULTS IN TERMS OF ACC AND F1 SCORE FOR HOUSE 2 OF THE REDD DATABASE.

Device	LSTM		CNN	
	ACC	**F1**	**ACC**	**F1**
Kitchen outlets	**99.65%**	99.48%	99.61%	99.48%
lighting	**91.58%**	**92.22%**	87.49%	89.13%
stove	99.57%	99.35%	99.57%	99.35%
microwave	92.87%	90.40%	**93.31%**	**91.20%**
Washer-dryer	100.00%	100.00%	100.00%	100.00%
Kitchen outlets	99.13%	98.70%	**99.37%**	**99.33%**
refrigerator	95.18%	95.18%	**95.30%**	**95.30%**
dishwasher	98.99%	98.49%	98.99%	98.49%

disposal	99.99%	99.99%	99.99%	99.99%
AVG	**97.44%**	**97.09%**	97.07%	96.92%

As can be seen in Table 2 the LSTM architecture slightly outperforms the CNN architecture reporting an accuracy of 97.44% (+0.37%) and an F_1 score of 97.08% (+0.17%) respectively. Specifically, it must be noted that all appliances accuracies are above 90% for LSTM setup, thus a very accurate estimation of ON/OFF states of appliances can be determined.

Based on the above the estimation of certain device can give indication of user presence within a household, especially three device groups must be distinguished. The first group consists of appliances, which are operating independently of user presence, e.g. fridges or stoves. The second group consists of devices which might operate on time control or the user might start them and then leave the house while they are operating, e.g. dishwasher or washing machine. The third group consists of devices, which are only operating with user control, e.g. the microwave or the disposal. Based on the above, user occupancy can be very well detected when focusing on the operation of appliances of the third group.

3.3. Multimedia Identification

Except the extraction of occupancy information, digital and especially multimedia related information is sensitive to residents' privacy as discussed in Section 2. The presented architecture in this Section deems to investigate the potential of identifying multimedia content using the aggregated energy consumption signal acquired outside the house from a smart meter installed after the main inlet of the household. The conceptual diagram of the architecture for identification of multimedia content explicitly using smart meter's energy data is illustrated in Fig. 6.

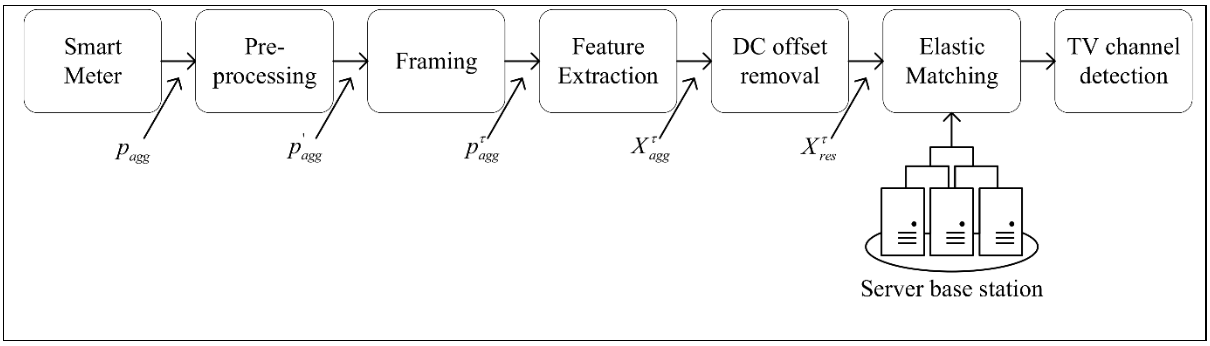

Fig. 6: Block diagram of the evaluated architecture for identification of multimedia content from a single smart meter using non-intrusive load monitoring.

The architecture illustrated in Fig. 6 consists of six steps, namely pre-processing, framing, feature extraction, DC offset removal, elastic matching and video channel detection. As can be seen in Fig. 6 a smart meter is measuring the aggregated energy consumption $p_{agg}(t)$. The aggregated signal is the sum of the energy consumption of all the devices within the house and in the present setup we consider the TV signal displaying a video as the target device with energy consumption $p(t)$ and all other home appliances having energy consumption $N(t)$, i.e.

$$p_{agg}(t) = p(t) + N(t) = p(t) + \sum_{i=1}^{M-1} n_i(t) \tag{12}$$

where M is the number of all appliances within the household, including the multimedia playing device (TV, monitor etc.) and the other devices, e.g. fridge, washing machine, operating in the considered household.

Subsequently, the aggregated signal, $p_{agg}(t)$, is frame blocked in frames of constant length equal to W samples p_{agg}^{τ} and transferred to a higher dimensional feature space resulting into $X_{agg}^{\tau} \in \mathbb{R}^{WxF}$ where F is the feature dimensionality. Furthermore, from every frame, the DC offset is removed, resulting to X_{res}^{τ}. The reason for the DC offset removal is the fact that the majority of the most common home appliances like fridges, refrigerators, boilers, electric heating bodies, electric ovens etc., consume energy at the order of 200-2000 Watts while the average energy consumption of monitor is at the order of 25-250 Watts. Therefore, the main part (DC part) of the energy consumption signal within each frame will come from devices with high energy consumption and by removing it in the remaining residual signal, $X_{res}^{\tau} \in \mathbb{R}^{WxF}$, the contour shape characteristics of the energy signal of devices with lower energy consumption like the TV or a monitor will be shown more clearly.

In order to find estimates for the multimedia in the measured signal X_{res}^{τ} an elastic matching function $g(\cdot)$ is used to compare the measured signal with a set of reference signals $R_m \in \mathbb{R}^{WxF}$ measured at a server base station as illustrated in Fig. 6 and described in Eq. 13.

$$Ch^{\tau} = \underset{1 \le m \le M}{\operatorname{argmin}} \{ g(X_{res}^{\tau}, R_m) \} \tag{13}$$

where Ch^{τ} is the estimated of the multimedia signal for the τ^{th} frame.

In order evaluate the investigated architecture the experimental setup and data of [19] is used and the estimation for a set of videos is performed using four different elastic matching algorithms, namely Dynamic Time Warping (DTW) [44], soft Dynamic Time Warping (sDTW) [44], Global Alignment Kernel (GAK) [45] and Multi Variance Matching (MVM) [46, 47]. In detail, two different monitors have been used separately for the measured aggregated signals X_{res} and the reference signals R_m for each of the M appliances. The results are illustrated in Fig. 7.

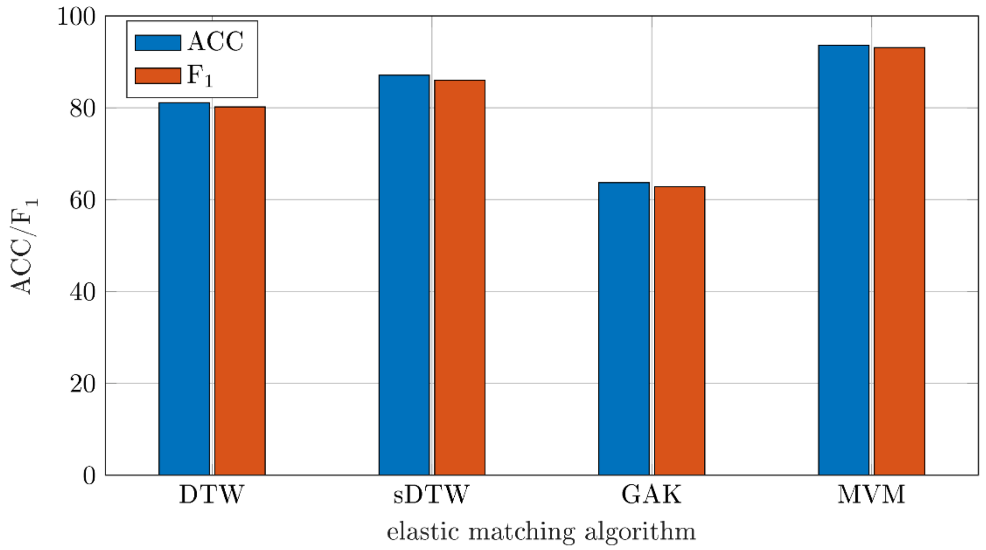

Fig. 7: Video Identification results for four different elastic matching algorithms and two different metrices.

As illustrated in Fig. 7 MVM outperformed all other elastic matching algorithms for both accuracy values as well as F_1 scores respectively, which is in agreement with our previous study [31] where MVM was also found to perform well on the NILM task. In detail, DTW, sDTW and MVM achieve accuracy and F_1 scores above 80%, significantly outperforming GAK with score around 60% respectively. Based on the results illustrated in Fig. 7 an extraction of multimedia information, and especially video signals, based on measurements of the aggregated energy consumption signal is feasible with high accuracy. For example, this information can be used to collect information regarding residents' preferences which is directly related to individuals' privacy and raises issues especially if this information about multimedia and/or TV channel watching preferences and their corresponding content are not monitored with given consent from the resident.

3.4. Socioeconomic Information

Apart from extraction of occupancy information as well as digital and multimedia related information also the socio-economic status of the residents of a household is sensitive information as discussed in Section 2. The presented architecture in this Section investigates the potential of extracting socio-economic and health related information, e.g. financial situation of a household or smoking habit, based on the aggregated energy consumption of a household. The evaluated architecture is shown in Fig. 8.

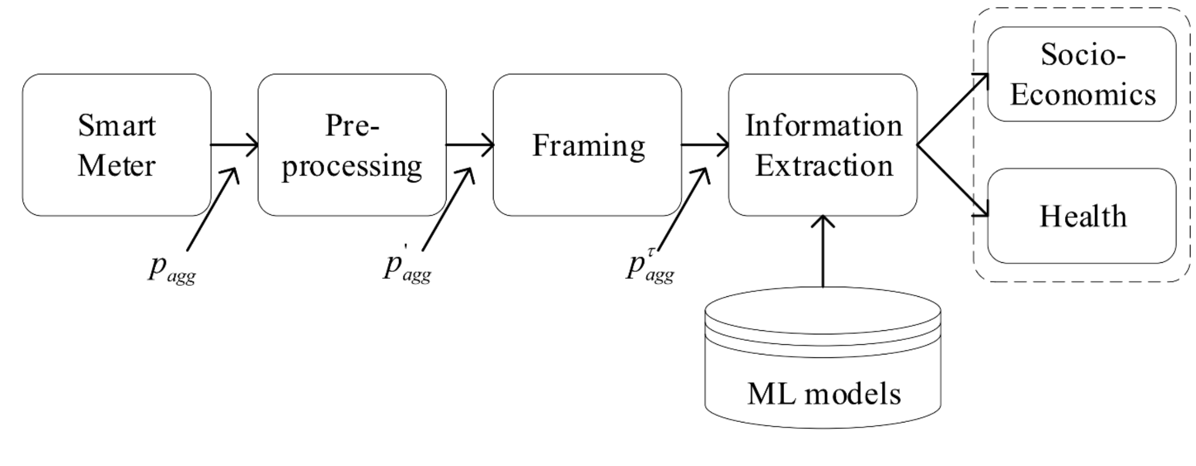

Fig. 8: Block diagram of the evaluated architecture for extraction of socio-economic and health-related information of the residents using a signal smart meter and non-intrusive load monitoring.

As illustrated in Fig. 8 the evaluated architecture consists of four steps, including smart metering, pre-processing, framing and prediction of socio-economic and health information. As can be seen in Fig. 8 a smart meter is measuring the aggregated energy consumption $p_{agg}(t)$, which is used as input to the machine learning model. The relationship between the input energy consumption p_{agg} and the socio-economic or health-related features can then be learned based on a set of labelled training samples $\{(p_{agg}^{\tau}, F^{\tau})\}$, with $\tau = 1, \ldots, T$, where F^{τ} denotes the τ^{th} sample of a socio-economic or health related feature, i.e. the average income of a household or the average age of the residents. Based on the above a machine learning regression model $r(\cdot)$ can be used to estimate the targets (socio-economic features) $r: p_{agg} \rightarrow F$ from the inputs (aggregated energy consumption signal) using an arbitrary loss function, e.g. MAE. The estimation of a feature can then be written as

$$\hat{F}_n = r(p_{agg}) \tag{14}$$

where $\hat{F}_m$ is the estimate for the n^{th} feature respectively.

For the information extraction stage two different machine learning algorithms have been utilized, namely a LSTM and a Bidirectional LSTM (BiLSTM) architecture [48]. The network structure of the two architectures is tabulated in Table 3.

TABLE 3: LAYER STRUCTURE OF LSTM AND BILSTM FOR EXTRACTION OF SOCIO-ECONOMIC AND HEALTH INFORMATION.

Layer number	LSTM	BiLSTM [48]
1	Input(336, 1, 1)	Input(336, 1, 1)
2	LSTM(128, sequences=True)	Conv1D(16, 4, padding='same', strides=1)
3	LSTM(256, sequences=False)	BiLSTM(128, sequences=True)
4	Dense(128, activation='tanh')	BiLSTM(256, sequences=False)
5	Dense(1, activation='linear')	Dense(128, activation='tanh')
6	-	Dense(1, activation='linear')

As illustrated in Table 3, both the LSTM and the BiLSTM architecture take input vectors of size 336 (one week of data with sampling rate of 30 min), while the core of the architectures consist of LSTM layers and BiLSTM layers respectively, with each architecture having a dense layer at the end using a linear activation function.

In order to evaluate the architecture, the 'SMinL' database [49] has been utilized as it is, to the best of the authors knowledge, the only database including socio-economic and health-related data together with the energy consumption data. In detail, the 'SMinL' database provides tagging for the categories: population, housing, finance, transport, environment, leisure time, digital, marketing, health, contact, safety, education, shopping, family and economy. The tagging is provided for 17 groups of households, which are referred to as ACRON groups. Specifically, for our evaluation the energy consumption data recordings of the complete year 2013 were used (year 2012 was not used as it has several gaps in the measurements), using 50 households per ACRON group, thus a total of 700 households. Furthermore we excluded ACRON-{B, K, M} as they have missing samples in the selected time interval. The list of evaluated ACRON groups including average values of properties of these groups is tabulated in Table 4.

TABLE 4: LIST OF AVERAGE PROPERTIES OF THE EVALUATED ACRON DATASETS WITH EACH ACRON-X DATASET CONSISTING OF 50 HOUSEHOLDS.

Dataset	Energy (kWh)	Avg. # Residents	Avg. Age	Avg. Income (k)	Avg. Beds	Avg. Value (k)
ACRON-A	4215	3.4	42.3	195	5.2	1321
ACRON-C	4772	2.7	46.5	117	3.9	599
ACRON-D	5200	3.0	32.7	148	3.1	1163
ACRON-E	4251	3.1	32.6	126	3.2	606
ACRON-F	3207	2.8	43.8	103	3.8	425
ACRON-G	3614	3.2	39.2	118	3.8	449
ACRON-H	3671	3.2	38.7	106	3.7	414
ACRON-I	3785	2.2	51.4	75	2.8	401
ACRON-J	3743	2.9	33.9	107	3.2	396

ACRON-L	3208	3.1	36.2	81	3.1	294
ACRON-N	3203	2.2	43.3	46	1.8	270
ACRON-O	2966	2.7	34.0	71	2.4	331
ACRON-P	2290	3.6	30.5	65	2.8	362
ACRON-Q	2671	2.6	33.7	46	1.9	312

As illustrated in Table 4 the ‘SMinL’ database covers a large variety in terms of energy consumption, average number of residents and their age as well as their financial situation, thus making it suitable for training generalized models for extraction ML based models for information extraction. Based on the above two different experimental setups have been evaluated, one with respect to evaluation of features related to socioeconomics and one with respect to health-related information. The description of the socio-economic as well as the health-related features are tabulated in Table 5.

TABLE 5: FEATURE DESCRIPTION FOR TEN SOCIO-ECONOMIC FEATURES AND SEVEN HEALTH-RELATED FEATURES DEPENDING ON THE ACRON GROUP OF THE “SMINL” DATASET (FOR DETAILED EXPLANATION SEE OF ALL FEATURES SEE [48]).

Socio-Economic Features	
residents age	being the average age of the residents
house size	being the average house size in square feet
house value	being the average house value
# residents	being the average number of residents
resident’s income	being the average income of all residents within one household
resident’s finance	being a rating of the financial situation of all residents
# cars	being the average number of cars per household
resident’s savings	being the average savings of all residents within one household
# children	being the average number of children per household
social class	being a rating of the social class as experienced by the residents themselves
Health-related Features	
smokers	being the average number of people smoking
exercise	being the average number of people that are frequently exercising
life change	being the average number of people who actively want to change their life-style
life standard	Being the average rating of the people’s life standard between 1 and 6
worries	being the average number of people, who are recently worried about their future
eating (fruits)	being the average number of people eating 3 or more fruits per day
eating (vegetables)	being the average number of people eating 3 or more vegetables per day

As can be seen in Table 5 the “SMinL” database provides a large variety for both socio-economic as well as health-related features making it suitable for evaluating the extraction of such features from the aggregated energy consumption data.

The results for ten different socio-economic characteristics are tabulated in Table 6, while the results for seven health related characteristics are tabulated in Table 7. Both have been evaluated in terms of normalized MAE and RSME as well as through the person correlation R.

TABLE 6: ESTIMATION RESULTS FOR LSTM AND BILSTM MODELS FOR TEN DIFFERENT SOCIO-ECONOMIC FEATURE CATEGORIES FOR THREE DIFFERENT PERFORMANCE MEASURES MAE, RMSE AND PEARSON COEFFICIENT

Category	LSTM			BiLSTM		
	MAE	RSME	Pearson R	MAE	RSME	Pearson R
residents age	0.081	0.109	0.133	0.075	0.099	0.278
house size	0.093	0.115	0.670	0.082	0.115	0.701
house value	0.138	0.184	0.725	0.101	0.132	0.827
# residents	0.074	0.090	0.426	0.060	0.092	0.422
resident’s income	0.141	0.176	0.777	0.109	0.127	0.785
resident’s finance	0.021	0.023	0.652	0.016	0.020	0.694
# cars	0.132	0.174	0.426	0.128	0.175	0.485
resident’s savings	0.077	0.092	0.766	0.054	0.066	0.863
# children	0.060	0.089	0.127	0.077	0.091	0.194
social class	0.067	0.079	0.762	0.062	0.074	0.775
AVG	0.088	0.113	0.546	0.076	0.099	0.602

As illustrated in Table 6 BiLSTM outperforms LSTM on average with a decrease of MAE (-0.012) and RMSE (-0.014) and conversely an increase of R (+0.056), as well as an improvement on all individual feature setups. Specifically, three different groups can be quantified according to their Pearson correlation R. First, these features showing R values significantly below 0.5, thus showing prediction values only slightly better than a naïve predictor. Second, these features reporting R values around 0.5, thus having a statistical significantly different prediction outcome than a naïve predictor. Third, these features having R values significantly above 0.5, thus having very accurate predictions for a specific feature.

In detail, for the results presented in Table 6 the prediction of the number of children and the age of the residents belongs to the first category. This might be due to the following reasons: The number of children might conflict with the number of residents, most likely it is not possible to estimate if a resident is a child or not due to similar patterns and common activities, i.e. children eat with their parents or parents washing their children’s clothes. Similarly, the residents age is difficult to obtain especially as the average age range is only between 30.5 and 46.5 (see Table 4), thus there are no household with very old residents or very young residents, which could explain the low accuracy score. Furthermore, number of cars and number of residents belong to the second category with R values of 0.485 and 0.422 respectively. Especially, the prediction of number of residents is probably confused by groupings of activities, i.e. couples or families might cook together or share the washing machine, similarly as with the prediction of number of children. Conversely, the number of cars is probably related to energy activities, e.g. the possibility of having a car available changes the behaviour of using electric appliances. Moreover, the third category especially contains features related to the house, e.g. house size or house value, and financial features, e.g. income, savings or social class. Most likely the good results can be attributed to two fundamental reasons. Frist, electrical energy consumption increases with house size and house value due to additional electrical appliances, e.g. more lighting. Second, different social classes and thus residents with different financial capabilities have different lifestyles, i.e. working habits or the fact how often the residents are going out for eating.

TABLE 7: ESTIMATION RESULTS FOR LSTM AND BILSTM ARCHITECTURES FOR SEVEN DIFFERENT HEALTH FEATURE CATEGORIES FOR THREE DIFFERENT PERFORMANCE MEASURES MAE, RMSE AND PEARSON COEFFICIENT

Category	LSTM			BiLSTM		
	MAE	RSME	Pearson R	MAE	RSME	Pearson R
smokers	0.120	0.157	0.735	0.109	0.153	0.775
exercise	0.059	0.077	0.714	0.053	0.066	0.806
life change	0.088	0.111	0.558	0.079	0.102	0.634
life standard	0.098	0.117	0.736	0.080	0.093	0.731
worries	0.075	0.094	0.311	0.069	0.085	0.353
eating (fruits)	0.098	0.126	0.749	0.087	0.116	0.823
eating (vegetables)	0.128	0.158	0.738	0.093	0.130	0.823
AVG	0.095	0.120	0.649	0.081	0.106	0.706

Similarly, as for the socio-economic features the average results for health-related features are better for the BiLSTM architecture compared to the LSTM architecture for all three performance measures: MAE (-0.014), RMSE (-0.014) and Pearson R (+0.057). Moreover, also the results on all feature categories are better for the BiLSTM architecture as well. In detail, using the same categorizations for performance measure as for the socio-economic features, there is only one health-related feature having a Pearson R score significantly below 0.5, being 'worries' and one feature having a Pearson R value around 0.5, which is 'life change'. This is probably due to the fact, that these two features are the only ones considers a feeling and not a measurable quantity, i.e. compared to the number of cigarettes someone is smoking. All other features show good Pearson R values around 0.8 for the BiLSTM, thus giving an accurate estimate. Specifically, four out of these five features are considering routines, e.g. smoking, exercising or eating, thus might be captured through daily routines in the energy signal, i.e. someone leaves always at the same time for the gym. Additionally, the life standard can be well predicted, which is probably due to correlation between life standard, value of the house and thus the energy consumption levels and trends in general.

Based on the above, it was shown that for both socio-economic as well as health-related features there are certain features that can be estimated very well based on the aggregated energy consumption signal, i.e. house value or residents' income, while there are some features that show poor performances when attempting to estimate them from the aggregated energy signal, i.e. residents' age or the number of children in a household. However, on average both socio-economic as well as health-related features can be extracted with accuracies well above those of a naïve predictor indicating that extraction of residents' information from the aggregated energy consumption signal is possible. In detail, for both socio-economic and health-related features BiLSTM reported better results for all accuracy metrices. The average Pearson coefficients for the ten socio-economic features was found equal to 0.602 and for the seven health-related features was found equal to 0.706, thus well above the naïve predictor.

4. Discussion and Conclusion

Based on the experimental setups and the results presented in Section 3, it was shown that the three most common techniques for processing the aggregated energy signal, namely load prediction, Non-Intrusive Load Monitoring and elastic matching, can be used to vastly exploit resident's information. First, based on load prediction and Non-Intrusive Load Monitoring, thus through the accurate ahead-prediction of energy samples and the event detection of certain devices, detailed occupancy information can be extracted from the aggregated signal when applying rules indicating resident's presence or absence. Second, based on elastic matching patterns within the aggregated signal can be matched with a set of reference signals and thus especially multimedia content, e.g. TV channels or video watching, can be identified. Therefore, user profiles in terms of genres or TV channel preferences can be created. Third, machine learning based model can be trained in order to estimate socio-economic and health related features of residents.

To summarize, it was shown that based on the aggregated energy consumption signal acquired from a smart meter outside the house privacy and security sensitive information related to the residents of a house can be extracted, such as occupancy information, multimedia watching and preferences as well as socioeconomic and health-related information. It can thus be seen that the measurements taken by energy smart meters do not only carry information about the levels of energy consumption but also about the preferences and behaviour of the residents of the household, which raises flags about privacy and security issues. Consequently, smart meters' information extraction must be protected/secured on hardware and software level, at the side of the meter as well as at the side of a server in the common case of transmission of measured data to the cloud, with smart meter data being encrypted when sent via a network. Detection models can also be used to detect if additional metering equipment is connected at the power inlet of the household in order to notice inference from fraudulent additional smart meters. The present evaluation has showed that security and privacy should be considered in the design of smart metering systems.

5. Acknowledgement

This work was supported by the UA Doctoral Training Alliance (https://www.unialliance.ac.uk/) for Energy in the United Kingdom.

References

[1] A. Cooper, “Electric company smart meter deployments: foundation for a smart grid,” *The Institute for Electric Innovation (IEI) Report*, 2016. [Online]. Available: https://www.edisonfoundation.net/iei/publications/Documents/Final%20Electric%20Company%20Smart%20Meter%20Deployments-%20Foundation%20for%20A%20Smart%20Energy%20Grid.pdf

[2] M. A. B. ShanZhou, “Smart meter deployment in Europe: A comparative case study on the impacts of national policy schemes,” *Journal of Cleaner Production*, vol. 144, pp. 22–32, 2017, doi: 10.1016/j.jclepro.2016.12.031.

[3] J. S. Vardakas, I. Zenginis, N. Zorba, C. Echave, M. Morato, and C. Verikoukis, “Electrical Energy Savings through Efficient Cooperation of Urban Buildings: The Smart Community Case of Superblocks' in Barcelona,” *IEEE Commun. Mag.*, vol. 56, no. 11, pp. 102–109, 2018, doi: 10.1109/MCOM.2017.1700542.

[4] S. Althaher, P. Mancarella, and J. Mutale, “Automated Demand Response From Home Energy Management System Under Dynamic Pricing and Power and Comfort Constraints,” *IEEE Transactions on Smart Grid*, vol. 6, no. 4, pp. 1874–1883, 2015, doi: 10.1109/TSG.2014.2388357.

[5] C. D. e. al, “A review on time series forecasting techniques for building energy consumption,” *Renewable and Sustainable Energy Reviews*, vol. 74, pp. 902–924, 2017, doi: 10.1016/j.rser.2017.02.085.

[6] C. K. Hyojoo Son, “Short-term forecasting of electricity demand for the residential sector using weather and social variables,” *Resources, Conservation and Recycling*, vol. 123, pp. 200–207, 2017, doi: 10.1016/j.resconrec.2016.01.016.

[7] J. Gao, E. C. Kara, S. Giri, and M. Berges, “A feasibility study of automated plug-load identification from high-frequency measurements,” in *2015 IEEE Global Conference on Signal and Information Processing (GlobalSIP): 14-16 Dec. 2015*, 2015, pp. 220–224.

[8] G. C. Koutitas and L. Tassiulas, “Low Cost Disaggregation of Smart Meter Sensor Data,” *IEEE Sensors Journal*, vol. 16, no. 6, pp. 1665–1673, 2016, doi: 10.1109/JSEN.2015.2501422.

[9] G. W. Hart, “Nonintrusive appliance load monitoring,” *Proceedings of the IEEE*, vol. 80, no. 12, pp. 1870–1891, 1992, doi: 10.1109/5.192069.

[10] Z. Li, T. J. Oechtering, and M. Skoglund, “Privacy-preserving energy flow control in smart grids,” in *2016 IEEE International Conference on Acoustics, Speech, and Signal Processing: Proceedings : March 20-25, 2016, Shanghai International Convention Center, Shanghai, China*, 2016, pp. 2194–2198.

[11] K. Buchanan, N. Banks, I. Preston, and R. Russo, “The British public’s perception of the UK smart metering initiative: Threats and opportunities,” *Energy Policy*, vol. 91, pp. 87–97, 2016, doi: 10.1016/j.enpol.2016.01.003.

[12] J. Zhao, J. Liu, Z. Qin, and K. Ren, “Privacy Protection Scheme Based on Remote Anonymous Attestation for Trusted Smart Meters,” *IEEE Transactions on Smart Grid*, vol. 9, no. 4, pp. 3313–3320, 2018, doi: 10.1109/TSG.2016.2626317.

[13] E. McKenna, I. Richardson, and M. Thomson, “Smart meter data: Balancing consumer privacy concerns with legitimate applications,” *Energy Policy*, vol. 41, pp. 807–814, 2012, doi: 10.1016/j.enpol.2011.11.049.

[14] R. Dong and L. J. Ratliff, “Energy Disaggregation and the Utility-Privacy Tradeoff,” in *Big data application in power systems*, R. Arghandeh and Y. Zhou, Eds., Amsterdam: Elsevier, 2017, pp. 409–444.

[15] F. Siddiqui, S. Zeadally, C. Alcaraz, and S. Galvao, “Smart Grid Privacy: Issues and Solutions,” in *21st International Conference on Computer Communications and Networks (ICCCN), 2012: July 30, 2012 - Aug. 2, 2012, Munich, Germany ; proceedings ; [including workshop papers]*, Munich, Germany, 2012, pp. 1–5.

[16] A. Ukil, S. Bandyopadhyay, and A. Pal, “Sensitivity inspector: Detecting privacy in smart energy applications,” in *Computers and Communication (ISCC), 2014 IEEE Symposium on*, Funchal, Madeira, Portugal, 6/23/2014 - 6/26/2014, pp. 1–6.

[17] G. Kalogridis, Z. Fan, and S. Basutkar, “Affordable Privacy for Home Smart Meters,” in *Ninth IEEE International Symposium on Parallel and Distributed Processing with Applications Workshops (ISPAW), 2011: 26 - 28 May 2011, Busan, South Korea ; proceedings ; [including joint conferences and workshops papers]*, Busan, Korea (South), 2011, pp. 77–84.

[18] Ulrich Greveler, Benjamin Justus, and Dennis Loehr, “Multimedia content identification through smart meter power usage profiles,” in *in Computers, Privacy and Data Protection (CPDP*, 2012.

[19] P. A. Schirmer, I. Mporas, and A. Sheikh-Akbari, “Identification of TV Channel Watching from Smart Meter Data Using Energy Disaggregation,” 2020. [Online]. Available: https://arxiv.org/pdf/2007.00326

[20] A. Kelati, J. Plosila, and H. Tenhunen, “Smart Meter Load Profiling for e-Health Monitoring System,” in *Proceedings of 2019 the 7th International Conference on Smart Energy Grid Engineering (SEGE 2019): August 12-14, 2019, Oshawa, Canada*, Oshawa, ON, Canada, 2019, pp. 97–102.

[21] F. Farokhi, “Review of results on smart-meter privacy by data manipulation, demand shaping, and load scheduling,” *IET Smart Grid*, vol. 3, no. 5, pp. 605–613, 2020, doi: 10.1049/iet-stg.2020.0129.

[22] T. Vafeiadis *et al.,* “Machine Learning Based Occupancy Detection via the Use of Smart Meters,” in *2017 International Symposium on Computer Science and Intelligent Controls - ISCSIC 2017: Budapest, Hungary, 20-22 October 2017 : proceedings*, Budapest, 2017, pp. 6–12.

[23] M. Jin, R. Jia, and C. J. Spanos, “Virtual Occupancy Sensing: Using Smart Meters to Indicate Your Presence,” *IEEE Trans. on Mobile Comput.*, vol. 16, no. 11, pp. 3264–3277, 2017, doi: 10.1109/TMC.2017.2684806.

[24] A. Allik, S. Muiste, and H. Pihlap, “Smart Meter Data Analytics for Occupancy Detection of Buildings with Renewable Energy Generation,” in *2020 9th International Conference on Renewable Energy Research and Application (ICRERA)*, Glasgow, United Kingdom, 9/27/2020 - 9/30/2020, pp. 248–251.

[25] C. Feng, A. Mehmani, and J. Zhang, “Deep Learning-Based Real-Time Building Occupancy Detection Using AMI Data,” *IEEE Transactions on Smart Grid*, vol. 11, no. 5, pp. 4490–4501, 2020, doi: 10.1109/TSG.2020.2982351.

[26] A. Albert and R. Rajagopal, “Smart Meter Driven Segmentation: What Your Consumption Says About You,” *IEEE Transactions on Power Systems*, vol. 28, no. 4, pp. 4019–4030, 2013, doi: 10.1109/TPWRS.2013.2266122.

[27] C. A. C. Montañez and W. Hurst, “A Machine Learning Approach for Detecting Unemployment Using the Smart Metering Infrastructure,” *IEEE Access*, vol. 8, pp. 22525–22536, 2020, doi: 10.1109/ACCESS.2020.2969468.

[28] D. Chen, D. Irwin, P. Shenoy, and J. Albrecht, “Combined heat and privacy: Preventing occupancy detection from smart meters,” in *IEEE International Conference on Pervasive Computing and Communications (PerCom), 2014: 24 - 28 March 2014, Budapest, Hungary*, Budapest, Hungary, 2014, pp. 208–215.

[29] C.-T. Pham and D. Mansson, “A Study on Realistic Energy Storage Systems for the Privacy of Smart Meter Readings of Residential Users,” *IEEE Access*, vol. 7, pp. 150262–150270, 2019, doi: 10.1109/ACCESS.2019.2946027.

[30] S. Balaji and S. Karthik, “Energy Prediction System Using Internet of Things,” in *2020 6th International Conference on Advanced Computing and Communication Systems (ICACCS)*, Coimbatore, India, Jun. 2020 - Jul. 2020, pp. 1131–1135.

[31] P. A. Schirmer, I. Mporas, and M. Paraskevas, “Energy Disaggregation Using Elastic Matching Algorithms,” *Entropy*, vol. 22, no. 1, p. 71, 2020, doi: 10.3390/e22010071.

[32] Matthias Pilz, Luluwah Al-Fagih and Eckhard Pfluegel, “Energy Storage Scheduling with an Advanced Battery Model: A Game–Theoretic Approach,” *Inventions*, vol. 2, no. 4, p. 30, 2017, doi: 10.3390/inventions2040030.

[33] M. Pilz, O. Ellabban, and L. Al-Fagih, “On Optimal Battery Sizing for Households Participating in Demand-Side Management Schemes,” *Energies*, vol. 12, no. 18, p. 3419, 2019, doi: 10.3390/en12183419.

[34] Matthias Pilz and Luluwah Al-Fagih, “A Dynamic Game Approach for Demand-Side Management: Scheduling Energy Storage with Forecasting Errors,” (in En;en), *Dyn Games Appl*, pp. 1–33, doi: 10.1007/s13235-019-00309-z.

[35] H. K. Nguyen, J. B. Song, and Z. Han, “Distributed Demand Side Management with Energy Storage in Smart Grid,” *IEEE Transactions on Parallel and Distributed Systems*, vol. 26, no. 12, pp. 3346–3357, 2015, doi: 10.1109/TPDS.2014.2372781.

[36] S. Welikala, C. Dinesh, M. P. B. Ekanayake, R. I. Godaliyadda, and J. Ekanayake, “Incorporating Appliance Usage Patterns for Non-Intrusive Load Monitoring and Load Forecasting,” *IEEE Transactions on Smart Grid*, vol. 10, no. 1, pp. 448–461, 2019, doi: 10.1109/TSG.2017.2743760.

[37] B. Liu, W. Luan, and Y. Yu, “Dynamic time warping based non-intrusive load transient identification,” *Applied Energy*, vol. 195, pp. 634–645, 2017, doi: 10.1016/j.apenergy.2017.03.010.

[38] C. Ju, P. Wang, L. Goel, and Y. Xu, “A Two-Layer Energy Management System for Microgrids With Hybrid Energy Storage Considering Degradation Costs,” *IEEE Transactions on Smart Grid*, vol. 9, no. 6, pp. 6047–6057, 2018, doi: 10.1109/TSG.2017.2703126.

[39] P. A. Schirmer, C. Geiger, and I. Mporas, “Residential Energy Consumption Prediction Using Inter-Household Energy Data and Socioeconomic Information,” in *2020 28th European Signal Processing Conference (EUSIPCO)*, 2020 (in press).

[40] N. Huang, W. Wang, S. Wang, J. Wang, G. Cai, and L. Zhang, “Incorporating Load Fluctuation in Feature Importance Profile Clustering for Day-Ahead Aggregated Residential Load Forecasting,” *IEEE Access*, vol. 8, pp. 25198–25209, 2020, doi: 10.1109/ACCESS.2020.2971033.

[41] Jean-Michel D., *Smart meters in London*. Kaggle. [Online]. Available: https://www.kaggle.com/jeanmidev/smart-meters-in-london

[42] P. A. Schirmer, I. Mporas, and A. Sheikh-Akbari, “Energy Disaggregation Using Two-Stage Fusion of Binary Device Detectors,” *Energies*, vol. 13, no. 9, p. 2148, 2020, doi: 10.3390/en13092148.

[43] M. DrIncecco, S. Squartini, and M. Zhong, “Transfer Learning for Non-Intrusive Load Monitoring,” *IEEE Transactions on Smart Grid*, p. 1, 2019, doi: 10.1109/TSG.2019.2938068.

[44] M. Cuturi and M. Blondel, “Soft-DTW: A Differentiable Loss Function for Time-Series,” 2017. [Online]. Available: https://arxiv.org/pdf/1703.01541

[45] M. Cuturi, “Fast Global Alignment Kernels,” in *Proceedings of the 28th International Conference on International Conference on Machine Learning*, 2011, pp. 929–936. [Online]. Available: http://dl.acm.org/citation.cfm?id=3104482.3104599

[46] L. J. Latecki, V. Megalooikonomou, Q. Wang, R. Lakaemper, C. A. Ratanamahatana, and E. Keogh, “Elastic Partial Matching of Time Series,” in *Knowledge Discovery in Databases: PKDD 2005*, 2005, pp. 577–584.

[47] Longin Jan Latecki, Vasileios Megalooikonomou Qiang Wang Deguang Yu, “An elastic partial shape matching technique,” *Pattern Recognition*, vol. 40, no. 11, pp. 3069–3080, 2007, doi: 10.1016/j.patcog.2007.03.004.

[48] J. Kelly and W. Knottenbelt, “Neural NILM,” in *BuildSys'15: Proceedings of the 2nd ACM International Conference on Embedded Systems for Energy-Efficient Buildings : November 4-5, 2015, Seoul, South Korea*, 2015, pp. 55–64.

[49] J.-M. D, *Smart meters in London*. https://www.kaggle.com/jeanmidev/smart-meters-in-london. Accessed: Oct. 22 2019. [Online]. Available: https://www.kaggle.com/jeanmidev/smart-meters-in-london